

Original papers

Internet of Things (IoT) for double ring infiltrometer automation



Ahmed A. Abdelmoneim^{a,c}, Andre Daccache^b, Roula Khadra^{c,*}, Mayank Bhanot^b, Giovanna Dragonetti^c

^a Department of Agricultural and Environmental Science, University of Bari, Piazza Umberto 1, Bari, Italy

^b Department of Biological and Agricultural Engineering, University of California Davis, One Shields Avenue, Davis, CA, USA

^c Mediterranean Agronomic Institute of Bari, Via Ceglie 9, 70010 Valenzano, BA, Italy

ARTICLE INFO

Keywords:
Soil variability
Precision agriculture
Irrigation
Infiltration
Microcontroller
Hydraulic conductivity

ABSTRACT

Double ring infiltrometer is a simple device used to measure water infiltration rate in the soil, one of the most important hydro physical characteristics and an essential parameter for various applications including: surface irrigation and drainage projects, infiltration or water purification basins, seepage losses at canals, soil leaching at waste storage sites. However, the high spatial variability of a soil makes a single point measurement rarely representative of an entire field. Nonetheless, Double Ring Infiltration tests are tedious, time consuming and require continuous attention, hence limiting the number of tests that may be performed simultaneously on a given site.

In the present research, an automated Internet of Things (IoT) double ring infiltrometer (DRI) is developed and validated in a loamy field. It consists of a DRI equipped with an ESP-32 microcontroller chip, a GPS module, a solenoid valve, a DIY conductance water level sensor, and a SD card module powered by a 12 V 11000mAh Li-ion battery charged by a 10 W solar panel. The double ring infiltrometer is designed to calculate the infiltration rate in real time, to store the data with the time stamp and geographical coordinates on an SD card or, to use a cloud service platform to upload the data over the internet. The aim is to facilitate soil infiltration mapping for precision agriculture and to build a soil infiltration inventory that could be used to continuously improve existing soil database.

The system was assembled and tested at nine different locations on a loamy soil experimental field. For validation, conventional (manually operated) tests were conducted at the same time. The system proved to be reliable ($R^2 = 0.99$), cost effective (115\$) and a hassle-free solution, ideal for multiple soil infiltration measurements.

1. Introduction

Infiltration rate is the process by which water on the soil surface penetrates the soil. It describes the capacity of a soil to absorb water (Mao et al., 2008). Quantifying soil infiltration rate and saturated hydraulic conductivity are keystone parameters for hydrological modeling, groundwater recharge/pollution, irrigation management, civil engineering, agricultural and non-agricultural drainage, and liquid waste disposal applications.

Soil infiltration is the major contributor in irrigation uniformity and application efficiency specially in surface irrigation. Furthermore, infiltration parameters are the major inputs in irrigation simulation models for water and solutes transportation.

In a typical infiltration event, the initial soil infiltration rate de-

creases with time. The rate of decrease slows down exponentially, and the infiltration rate reaches a steady state called basic infiltration rate, which is equal/very close to the soil hydraulic conductivity. In highly permeable soils, reaching the basic infiltration rate could take up to 6 h (Johnson, 1963). Soil infiltration rate and cumulative infiltration are related by the equation:

$$i = \frac{dz}{dt} \quad (1)$$

where i is the infiltration rate in mm/h, z is the infiltrated depth in mm and t is time in h.

The rate of decrease to reach the basic infiltration rate is affected by a number of factors including initial soil moisture content, soil texture and structure, topography, soil surface cover conditions, aggregate stability,

* Corresponding author.

E-mail address: khadra@iamb.it (R. Khadra).

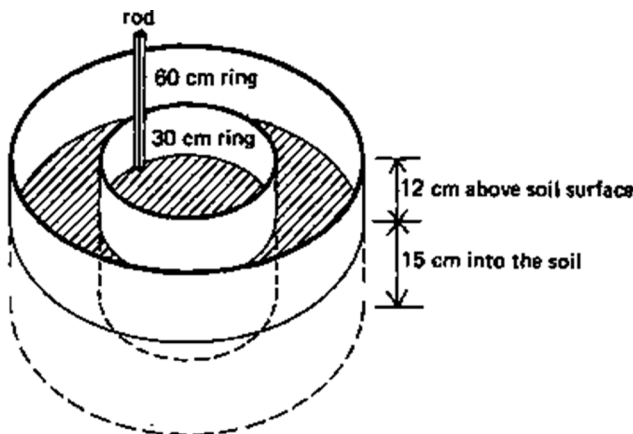


Fig. 1. Setup of a Double Ring Infiltrometer (Brouwer et al., 1988).

cracks and crusts, water quality (Dragonetti et al., 2020; Gang and Xiangyun, 2008). Yet, soil is not a homogenous medium and the majority of the above-mentioned factors could show a significant spatial variability even in small sized fields (0.1–2 ha) (Leonard and Andrieux, 1998).

Another usually neglected factor is the variation in soil surface structure during an infiltration event. The soil infiltration rate is

significantly impacted by the changes in the soil surface conditions affected by the disintegration of soil aggregates, surface seal formation and formation of air pockets inside the soil (Green, 1962).

There are several methods to estimate soil infiltration rate in the field, depending on the water application method, modelling theory, and final objectives. One of the most common used devices to measure vertical infiltration is ring infiltrometers under constant and falling head methods.

In this study, a low cost automated Internet of Things (IoT) double ring infiltrometer was developed and validated in the field. The prototype uses a DIY water level sensor composed of 4 graphite electrodes to sense the water connectivity and calculate the soil infiltration via ESP32 microcontroller when the water level falls below two consecutive electrodes. Automation facilitates soil infiltration mapping and overcomes the impracticality of traditional DRIs.

1.1. Ring infiltrometers

The simplicity of a ring infiltrometer made it the most widely used technique for soil water infiltration measurement. In its simplest form, the ring infiltrometer consists of a cylinder with a known diameter (usually 30 cm) inserted vertically into the soil surface. Water is ponded inside the cylinder and the rate of infiltration is measured by monitoring water level change with time, using a ruler and a stop watch.

The Double Ring Infiltrometer (DRI) was developed to minimize the

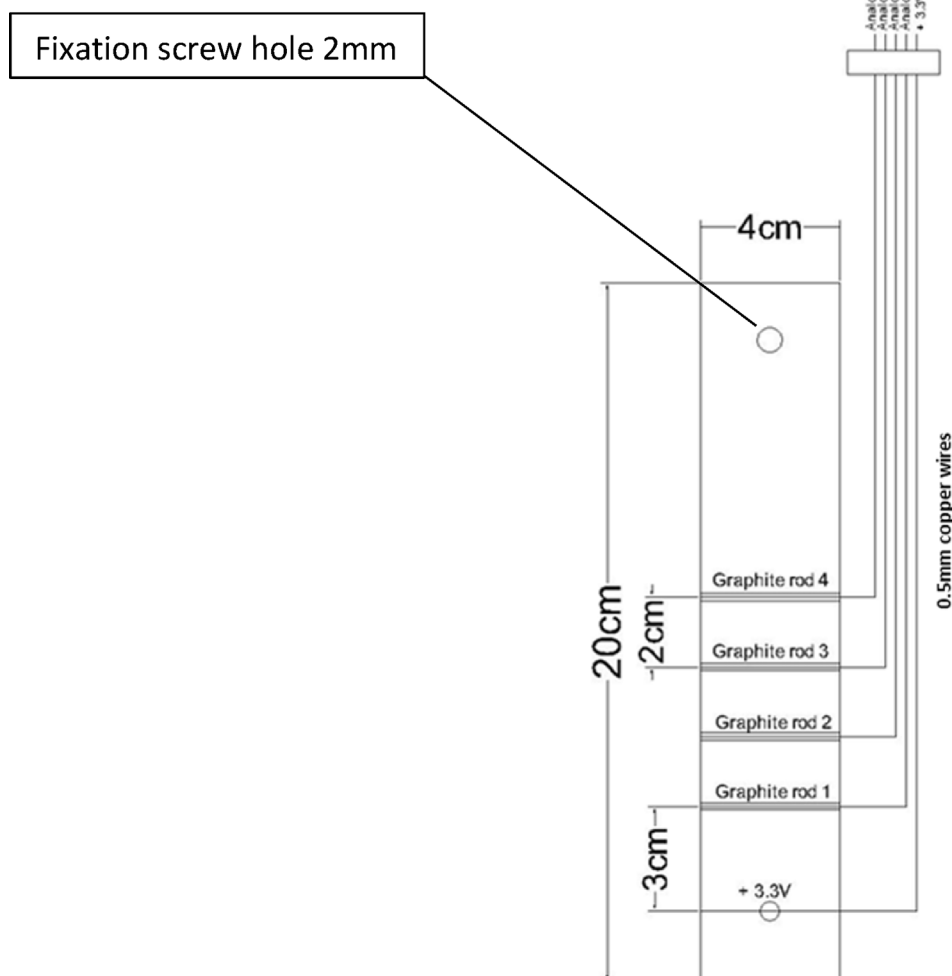


Fig. 2. Schematic diagram of the developed water level sensor.

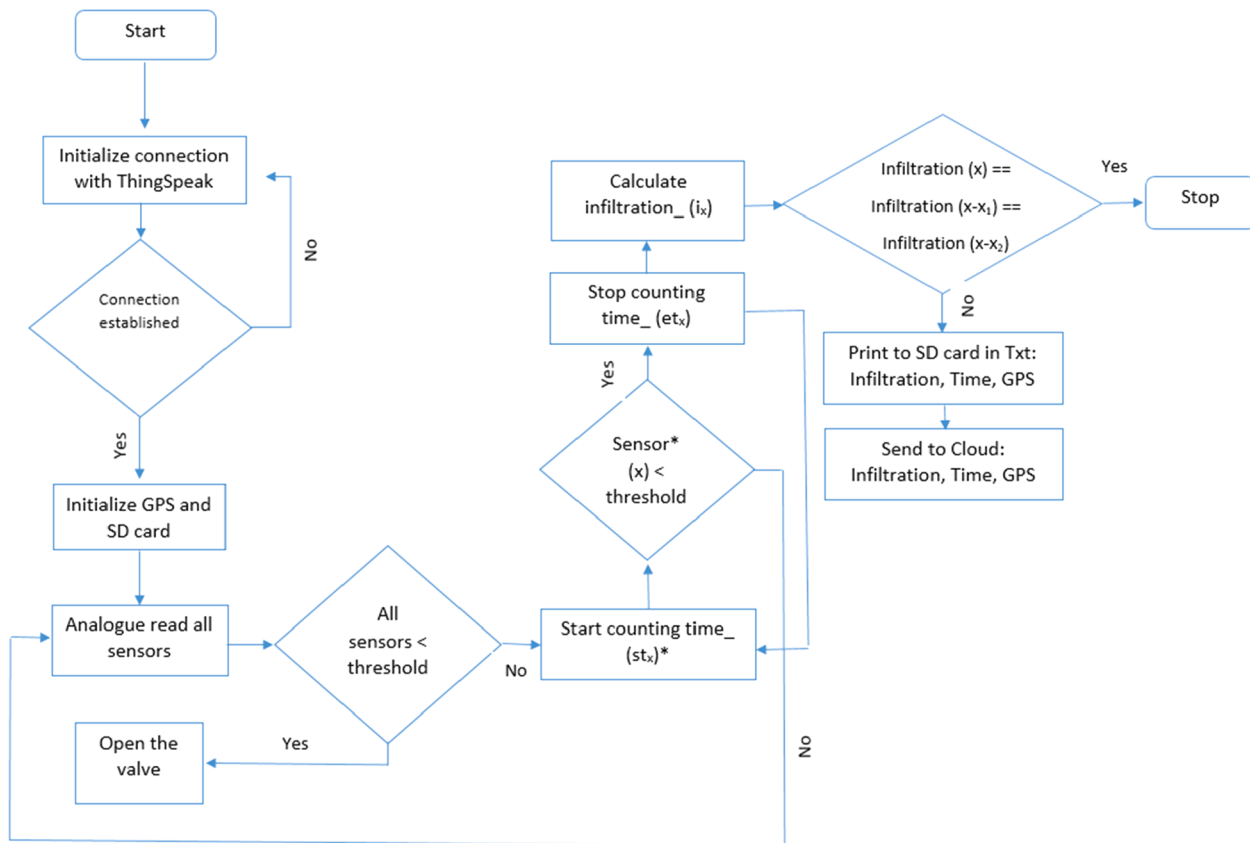


Fig. 3. Algorithm flowchart: * (x) refers to the sensor number, (st_x) Start time for each sensor, (et_x) End time.

impact of horizontal infiltration error introduced by single ring infiltrometers. By adding water between the two rings, the measurements are restricted to one dimensional flow. The standard method (ASTM, 2018) consists of two open cylinders 60 and 30 cm, both manually inserted 15 cm under the soil surface. The water is poured in the inner ring to a known height while adding water between the rings simultaneously. The decrease in water level inside the inner ring is measured as a function of time. As the ring dimensions are fixed, variation of water level in the inner ring represents the infiltration rate in mm/h (Fig. 1).

There are two concepts for water application to the DRI, either by 1) falling head: adding water to a fixed level (between 5 and 10 cm), registering the rate of decrease with time, and then resupplying once needed, to the assigned level. 2) constant head: adding water to a fixed level and sustaining it using a large Marriott reservoir; in this latter case, the infiltration rate will be the variation in volume needed to maintain a certain constant ponding level in the inner-ring of the DRI over time, making it a less laborious process (Reynolds et al., 2002).

Sandoval et al. (2017) compared constant head to falling head permeability tests using different porosity mediums in the laboratory. The falling head permeability test showed high dispersion and was not sensitive to changes in porosity compared to constant head, with standard deviations (StdDev) ranging from 0.98 to 1.46 for different mediums, while the constant head showed better results for the same mediums with StdDev ranging between 0.5 and 1.14.

One of the main disadvantages of using DRI, is the possible disturbance of the soil structure leading to either compression or cracking, which can impact the measured infiltration rate. In addition, the dimensions of the rings could impact the results in particular cases. Lai and Ren (2007) measured saturated hydraulic conductivity at seven sites using four different sizes of DRIs with inner ring diameters (20, 40, 80 and 120 cm). Detailed numerical investigations were also conducted to explain how the inner-ring size of a DRI influences the measured

hydraulic conductivity in a heterogeneous soil. Field and simulation results both demonstrated that the variability in measured hydraulic conductivity was greater for smaller inner rings in (e.g., inner diameter < 40 cm), and gradually decreased as the ring size increased. Li et al. (2019) confirmed the previous conclusion by performing 190 DRI tests using inner rings dimensions (15, 20, 25, 30 and 40 cm), the results also indicated that the increase of the infiltrometer inner diameter would weaken the influence of the infiltrometer scale effect.

Furthermore, DRI tests require considerable time and efforts to be performed properly. Water level change needs to be recorded every short time step (1–10 min) during the first hour of the test, specially when the infiltration rate of a dry soil is high. As the infiltration speed slows down, water level readings will be reduced to 20–30 min in the second hour and to each 60 min for the rest of the test after that. On highly permeable soil, the test could last for up to 6 h to reach steady state with even more frequent readings (Johnson, 1963). This tedious operation requires at least two dedicated operators for water level observation and for the manual registration, thus making the entire measurement subjected to human error and data loss, especially during the first hour of the test, where the initial infiltration rate is relatively high and the measurement time step is short.

Different references reported different recommended initial time steps for the first hour that ranged from 1 to 10 min (ASTM, 2018; Brouwer et al., 1988; Mao et al., 2008; Youngs, 1987). Yet not reported a justification for the selected time step. Zhang et al. (2017) performed an extensive study to investigate the impact of the initial measurement time step on the resulted error. The study reported the impracticality and operational difficulties of using a very short time step such as (1–2 min) which will produce a high measurement error and suggested using longer steps (5–10) min as long as the measured average infiltration rates are positioned at the midpoint. Such results emphasise the importance of using an automated reading mechanism.

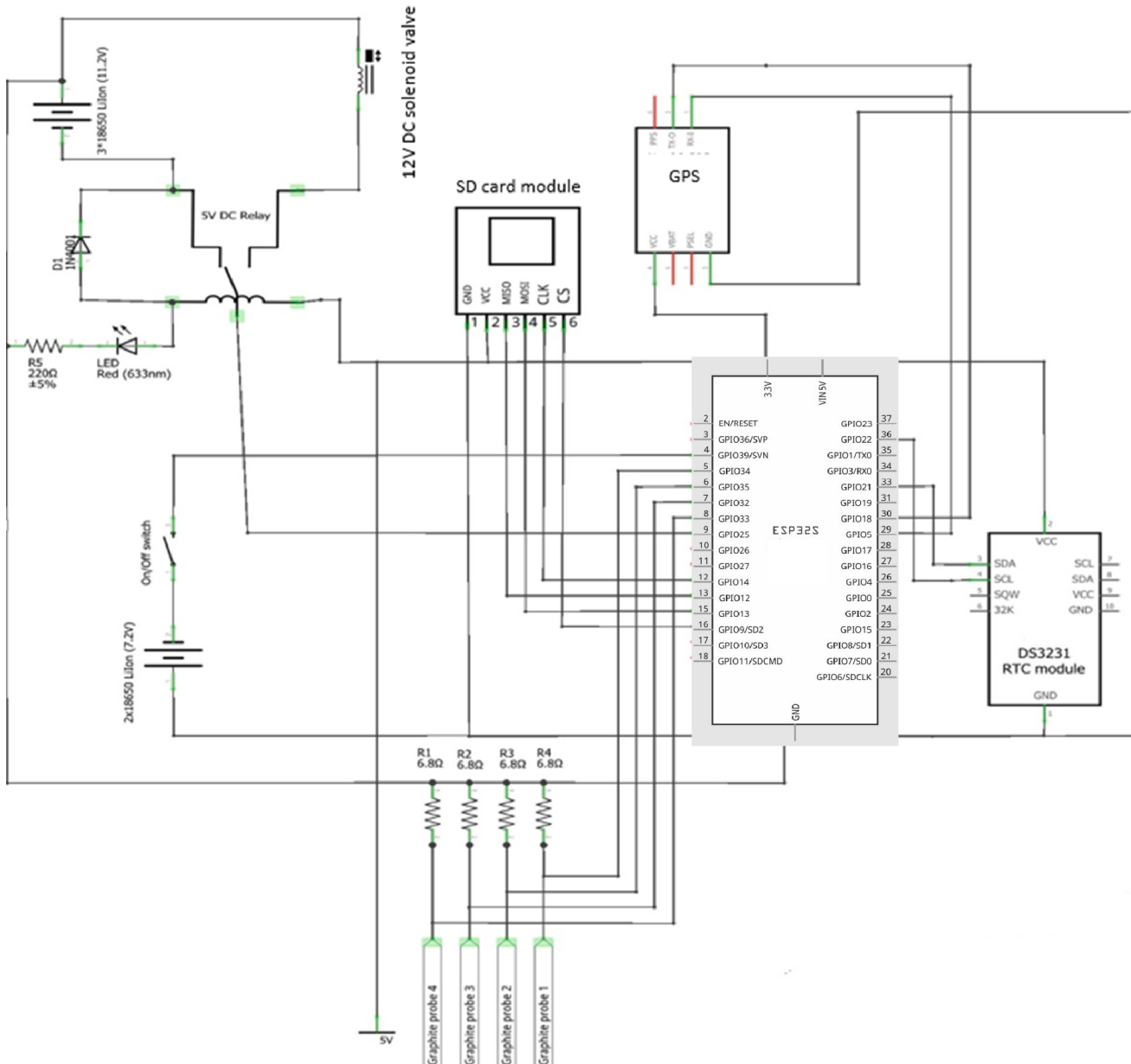


Fig. 4. Connection scheme frizzing open source software <https://fritzing.org>.

1.2. Automation of ring infiltrometers

A number of prototypes were developed, to in situ automate the infiltration tests and overcome the above-mentioned limitations. These prototypes used both falling and constant head concepts. One of the earliest models was developed by (Constantz and Murphy, 1987) using a Marriott bottle coupled with a flow meter designed to present the variation in water level as a function of internal gas pressure variation. The relation between the internal gas pressure and flow was measured by attaching a pressure transducer to the ceiling of the Marriott bottle and monitoring gas pressure changes during outflow with a programmable data logger. Following this concept, Priksat et al. (1992) enhanced the prototype by adding another pressure transducer in the bottom and a bubble tower, incrementing the precision of water height measurement ($\text{StdDev} = 2.2 \text{ mm}$) compared to height measurements made with only one transducer ($\text{StdDev} = 6.2 \text{ mm}$). Yet, those prototypes required continuous attention and manual water level control once the bottle chamber is empty, thus they cannot be described as fully

automated.

The earliest constant head automated DRI prototype was developed by Maheshwari (1996). A water level sensor consisted of three electrodes (common, upper water level and lower water level) installed inside the double ring infiltrometer. When the water level drops below a pre-set value (5 mm) the sensor sends a signal to the computer which instructs a solenoid valve to open and fill the ring from an elevated tank, until the water level returns to the original state. The infiltration is measured through calculating the variation in water level in the tank with time. The setup required a continuously connected laptop equipped with a user-friendly software to initiate the test, store the time, store water level changes, and calculate the infiltration.

At a cost of 200\$, Milla and Kish (2006) developed an automated DRI using two infra-red (IR) water level sensors and BX-24 microcontroller that uses Atmel AT90S8535 microprocessor. The prototype was capable of measuring infiltration and store it on the microcontroller to be downloaded by the user.

Arriaga et al. (2010) automated the traditional falling head

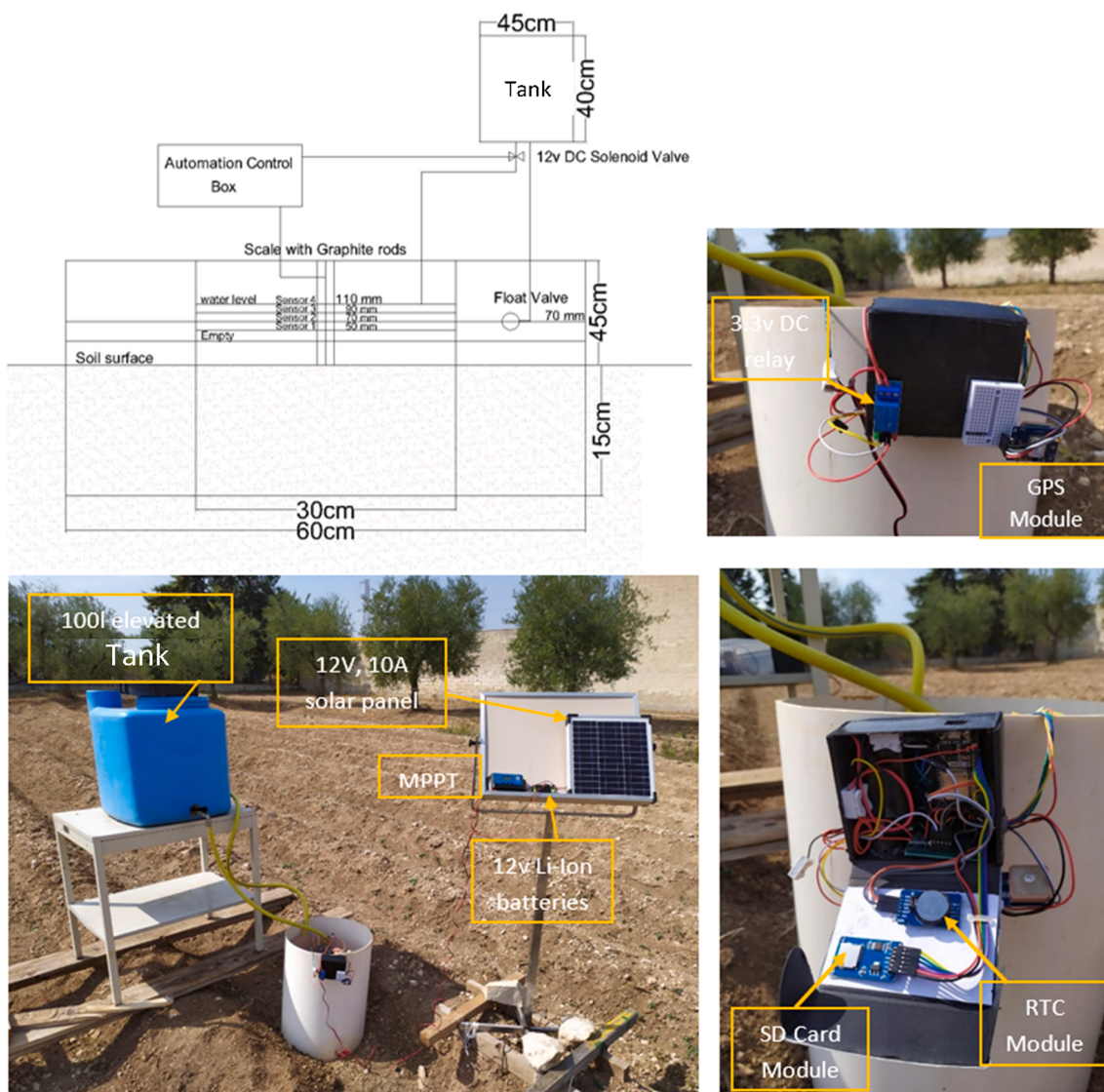


Fig. 5. Setup sketch and prototype in the field.

procedure described by Reynolds et al. (2002) and developed an automated DRI using transducers and data logger. Two holes with 3.8 cm in diameter were drilled in the rings body and fine tubes (0.63 cm diameter) were inserted through the holes. The outside end of the tube was connected to a transducer while the inside end was wrapped with a permeable cloth sheet to avoid clogging with debris. Fatehnia et al. (2016) Used Arduino Uno Microcontroller with a peristaltic pump, Hall Effect sensor and a commercial eTap water level sensor along with a locally assembled MOSFET transistor sensor to develop an automated system. The pump was used to fill the inner ring while the hall sensor measured the water velocity and the eTap recorded the variation in water level. All data were analyzed by a microcontroller depending on its internal time function and stored on a micro-SD-card. The system performed reliably; however, the eTap sensor suffered from drifting due to temperature sensitivity while the MOSFET sensor was able to read just the water contact event, thus the system relied on the eTap to measure the infiltration.

Although some of the mentioned systems are satisfactory and reliable, yet none found in the literature considered the developing of an IoT-DRI capable of uploading the results into an accessible infiltration library. In a high spatially variable feature such as soil infiltration (Bautista and Wallender, 1985) developing an automated geo-referenced measurement device is crucial. Having the possibility to

store all the geo-referenced infiltration tests on a public/private website to be used by operators/farmers/researchers, will facilitate farm management as long as creating many research opportunities from the generated and continuously enriched database with infiltration measurements.

The Internet of Things (IoT) refers to uniquely identifiable smart devices/objects connected to the internet that can sense data, react with their environment and send the data into a web platform. Coupled with cloud computing, IoT is the driving engine of Artificial Intelligence (AI) and robotics into farming, both in large commercial and consumer level scales (Mohanraj et al., 2016).

Advances in electronic technologies have provided researchers the access to low-cost, solid-state sensors and programmable microcontroller-based circuits. This interprets the fast growing attention given to IoT in agriculture in the last 5 years. García et al. (2020) did an extensive literature review of the IoT Systems prototyping for Irrigation in precision agriculture both as hardware microcontrollers (MCU) utilized and service web platform. Out of 160 studies, 80% were performed in the three years previous to the study (2017–2018–2019). The authors also found That ThingSpeak was the most identified service web platform used in research studies, while Arduino Uno MCU was the most utilized prototyping microcontroller especially for applications that do not require Wireless Sensors Networks (WSN).

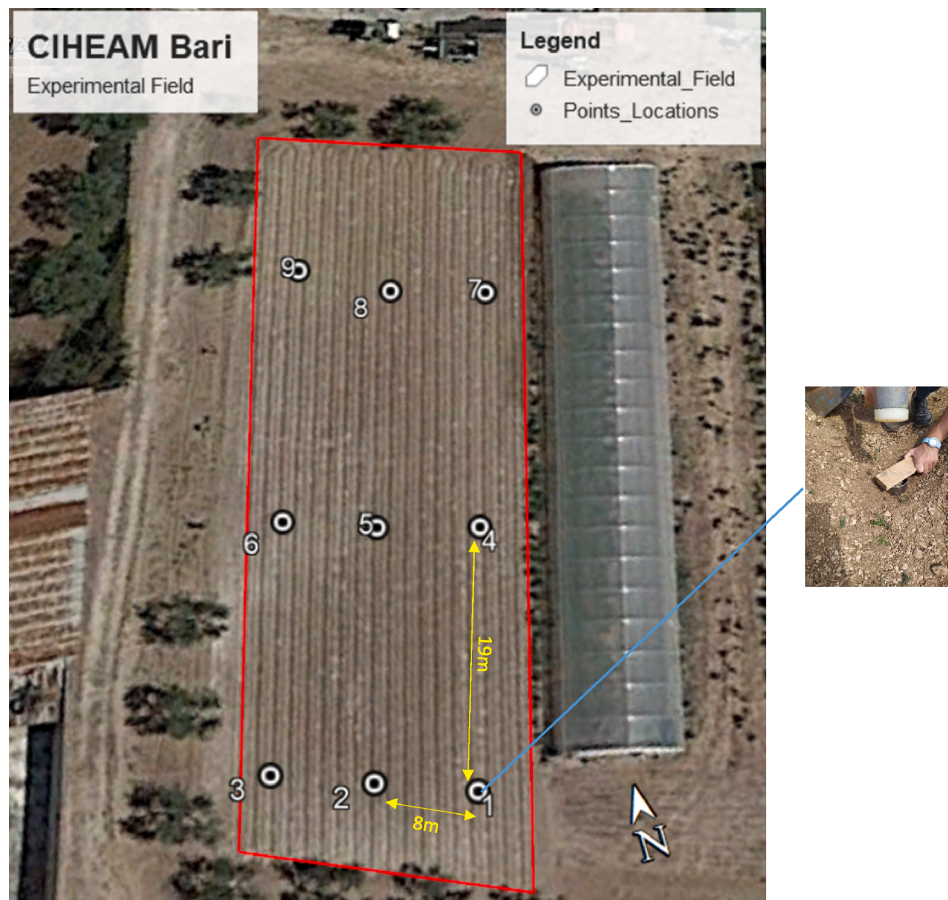


Fig. 6. The 9 measurements' sites as generated by the prototype.

Table 1
Soil physical properties: texture, SWC, bulk density and stone mass percentage.

	n. sample	INITIAL SWC (%)	Bulk density (g/cm^3)	Particle size distribution Sand (%)	Clay (%)	Loam (%)	Texture class	Stone mass percentage in soil (%)
Head	Point 1	3.84	1.283	46.6	14.5	39.2	loam	32
	Point 2	3.43	1.347	46.74	14.08	39.18	loam	30
	Point 3	3.11	1.251	46.64	14.31	39.13	loam	32
Middle	Point 4	7.49	1.188	43.18	14.20	42.67	loam	36
	Point 5	8.39	1.145	42.40	14.50	43.10	loam	33
	Point 6	8.99	1.170	42.39	14.42	43.19	loam	38
Tail	Point 7	5.20	1.154	44.69	14.99	40.32	loam	32
	Point 8	6.47	1.251	45.06	15.06	39.89	loam	27
	Point 9	5.66	1.202	44.8	15	40.2	loam	30

The aim of this work is: 1) to develop a low-cost falling head IoT geo-tagged DRI device capable of measuring and cloud storing soil infiltration rate. 2) To test and field validate the new prototype in the field, and 3) finally to perform a field infiltration mapping.

2. Development of the prototype

The IoT-DRI is a geo-tagged, falling head, automated infiltrometer. It can measure infiltration through a water level sensor with four electrodes 2 cm distanced (Fig. 2). When the water level drops at any electrode, the time is stored on the MCU through the real time clock (RTC). When the water level drops below two consecutive electrodes, the infiltration is calculated and printed as a text file saved on an SD card. Furthermore, the results are sent to be plotted on a cloud service website using the Wi Fi capability of the ESP32 and the API field key provided by the cloud service platform (Thing Speak). The data could be

downloaded in .CSV format for allowed users or designated as open access. Once the water level in the inner ring drops under the last bottom electrode, the ESP32 microcontroller sends a signal to open a solenoid valve connected to an elevated tank, to fill the inner ring and re-set the water level to the top electrode level. Fig. 3 illustrates the code algorithms written with C++ programming language.

The infiltration is calculated as a function of the time needed for the water level to drop below two consecutive electrodes. Thus the four electrodes' sensor allows for three infiltration measurements in each cycle before starting the filling event. This feature will allow future research on the impact of pressure head decrease on the infiltration rate in different soil textures/structures.

ESP32-WROOM-32 is a low cost powerful microcontroller module with an integrated WiFi and dual-mode Bluetooth. It targets a wide variety of applications, ranging from low-power sensor networks to the most demanding tasks. At the core of this module is the ESP32-D0WDQ6

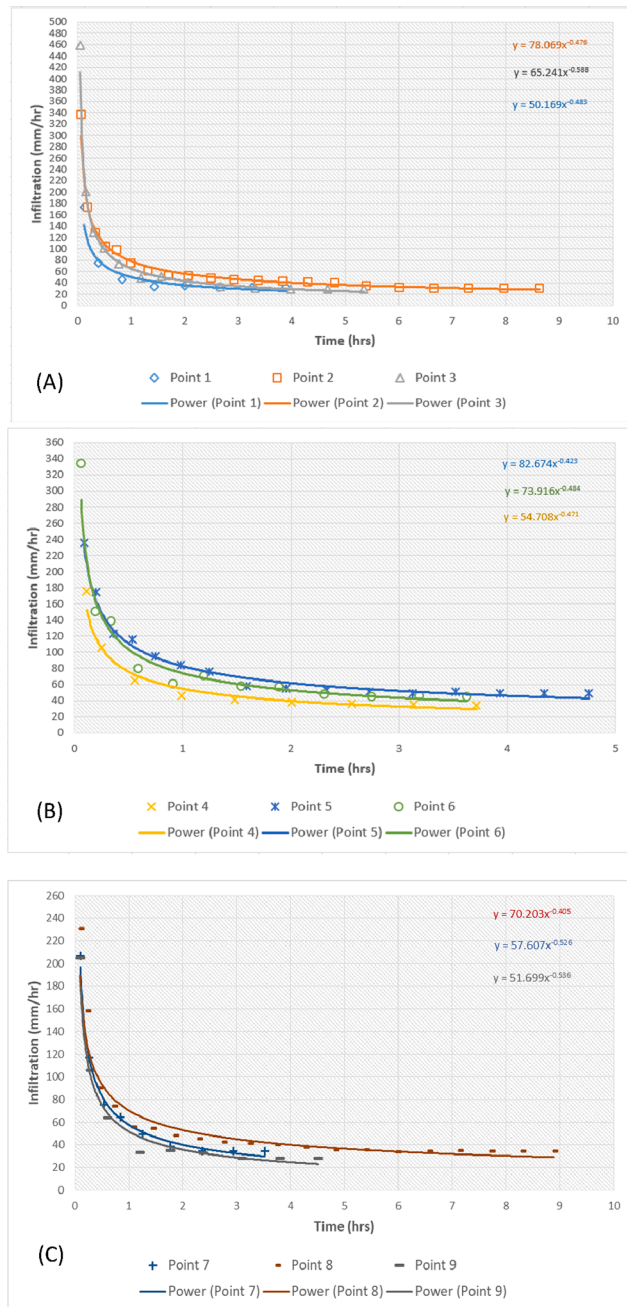


Fig. 7. Infiltration curves in the Head (A), Middle (B) and Tail (C).

chip with a dual core or single core LX6 microprocessor that operates the voltage range of 2.2 to 3.6 V. It has a 448Kbyte Data ROM and 512 Kbytes Data SRAM (Banerjee et al., 2020). Engineered for mobile devices, wearable electronics, and IoT applications, ESP32 achieves ultra-low power consumption through power saving features including fine resolution clock gating, multiple power modes, and dynamic power scaling. In this study the ESP32 is connected to a real time clock module, SD Card reader, Gy-GPS Neo6m and powered by 2Li-Ion batteries.

ThingSpeak™ is an IoT analytics platform service that allows for aggregating, visualizing and analyzing live data streams in the cloud (Pasha, 2016). In this study, the platform was used as a tool for visualizing and publishing the collected data. However, the user could execute MATLAB® code to perform online analysis and processing of the data. ThingSpeak is often used for prototyping and proof of concept IoT systems that require analytics.

The design of the system consists of the ESP32, a real time clock

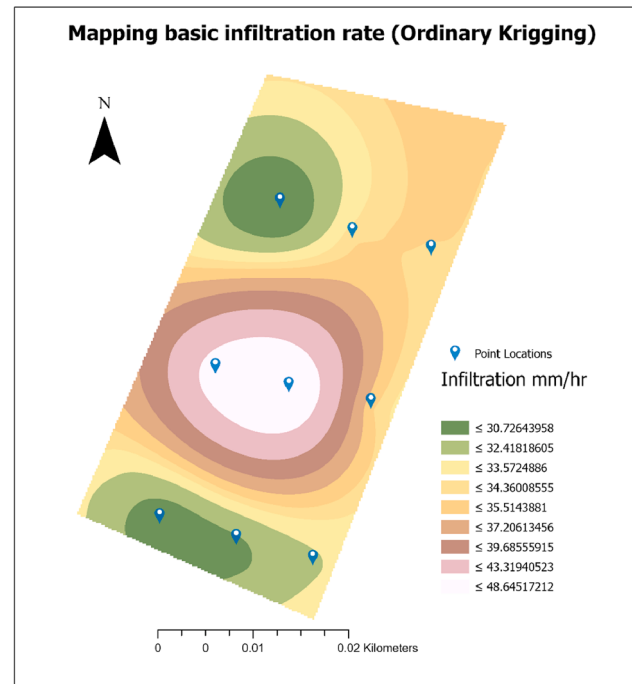


Fig. 8. Interpolated map of basic infiltration rate in the experimental field using IDW.

(RTC), a micro- SD card reader, Neo6m GPS module, two Li-Ion batteries providing 7.2 V and a water level sensor. The scheme and connections are presented in Fig. 4.

Graphite was selected because it is an excellent conductor to be used as an electrode as it does not oxidize and dissolve like other metals due to electrolysis when electrical current is applied. The 4 graphite electrodes on the ruler are connected to 4 analog pins on the MCU via 1 mm copper wires while the fifth wire is connected to the 3.3v supply pin. The dimensions of the DRI could vary from one case to another but in all cases the bottom of the scale should touch the soil surface after installing the inner ring in the field to allow the positive pole to be always in contact with moisture. The water level sensor was calibrated in the lab by measuring the corresponding water height to the recorded readings.

A 12 V ½" DC solenoid valve (Baco Engineering, model: p0018) was connected to a 100L elevated tank (1 m from the ground). The size of the tank was selected to support the expected required volume of water in sand families for 6 h using the USDA Natural Resources Conservation Service (soil intake family 2.0) (Walker et al., 2006). In the output end of the valve, a strainer was added to dissipate the pressure of the flow to have minimal impact on soil structure while filling. The dimensions of the tank are (40 * 40 * 45 cm). The valve is controlled by the MCU using an electromagnetic 5v DC relay and supplied by 3 rechargeable 16,850Li-Ion batteries. The batteries are being charged with a 12 V solar panel system via charging controller, allowing for sustainable charging for continuous operation (Fig. 5). A float valve was connected directly to the tank to keep the water level in the outer ring (between the rings) at 80 mm. The outer ring is a 60 cm in diameter while the inner ring is 30 cm.

The GPS module was programmed to start establishing the connection since the start of the system, however it will not print the location coordinates to the SD card until 10 min of the last switch on. The reason is that it could take some time in certain locations to connect at least to three satellites. The code was written using open-source Arduino software IDE 1.8.13 (<https://www.arduino.cc/en/>) and uploaded to the ESP32 MCU. The setup sketch and the prototype are presented in Fig. 5.

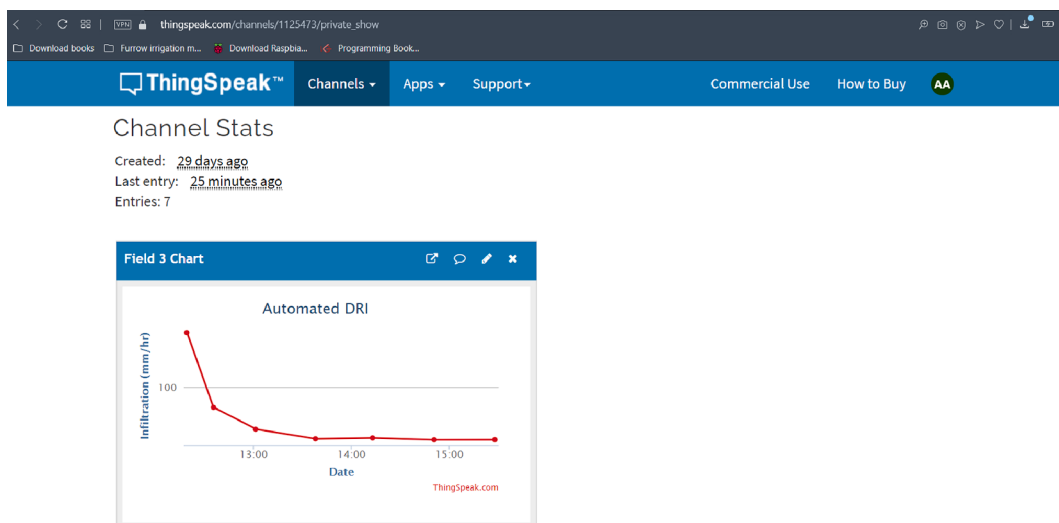


Fig. 9. Infiltration curve of point no. 1 as shown on ThingSpeak platform.

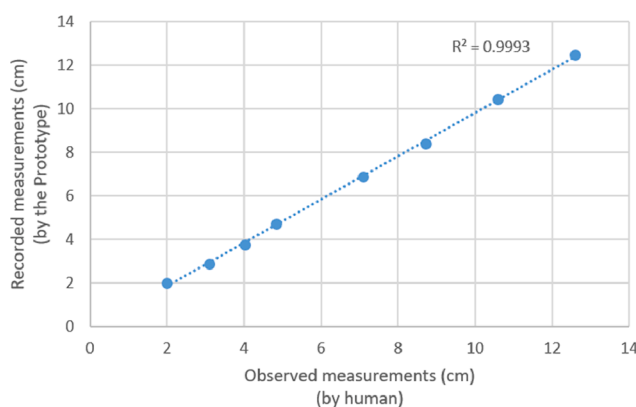


Fig. 10. Comparison between the measured cumulative infiltration and the corresponding recorded data.

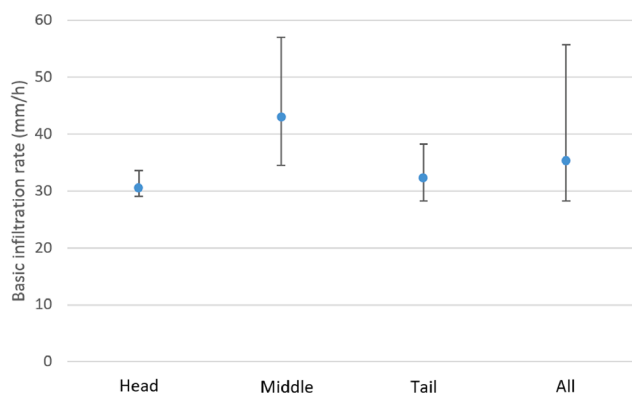


Fig. 11. Variation of Basic infiltration rate in the head, middle and tail of the field.

3. Validation and evaluation in the field

The trials were performed in 9 different locations in CIHEAM Bari experimental field (20 m * 50 m) – Italy (Fig. 6). The locations were selected to cover the head, middle, and tail, of a furrow-irrigated field to be used for infiltration mapping.

The initial soil moisture content, bulk density and soil texture were

measured in the nine locations to investigate the correlation with the resulted infiltration.

Soil moisture content is the main feature effecting the soil matric potential gradient (Hino et al., 1988). The high initial soil infiltration rate is mainly due to the relatively high matric potential gradient of an initially dry soil. The soil suction gradient decreases with the increase of wetted soil depth. Thus, it is important to estimate the initial soil moisture content in the field prior to mapping the infiltration, to value the main drivers for spatial variability if existent. The initial soil moisture content was measured gravimetrically by burning the samples on 105 °C in the oven for 24 h.

Bulk density is defined as the dry weight of soil per unit volume of undisturbed soil. Bulk density can be used to give an indication of the porosity, degree of compaction and structure of the soil. Higher bulk density indicates higher compaction thus lower infiltration capacity (Resch and Wahbi, 2016). The measurement of soil bulk density was performed by collecting undisturbed soil samples in the 9 points through inserting a standard metal ring with known volume into the soil, then determining the weight of the collected soil after drying on 105 °C for 24 h.

Validation of the prototype was performed in three points (1, 5 and 9) by comparing the observed and registered infiltration rates using a stopwatch and a ruler while the prototype is functioning. Basic infiltration zones were generated using ordinary kriging interpolation and ArcPro GIS. Finally, further statistical investigation for the impact of the mapped soil properties on the infiltration spatial variability was performed.

4. Results

The system was used in 9 different locations representing head, middle and tail of the field. The soil of the experimental field is loamy, characterized with high percentage of gravel ranging between 27 and 33% and a bulk density around 1.2 gm/cm³ (Table 1). The soil prior to the tests was relatively dry with initial soil moisture content (SWC) varying between 3 and 9%, and a basic infiltration rate ranging between 28 and 34 mm/h. The time to reach the basic infiltration rate was around 5–9 h with a steep reduction of 60–70% in the first 30 min, and a very low reduction in the following hours, except for two points (5 and 6) in the middle of the field. The generated infiltration curves of all points are illustrated in Fig. 7.

With the GPS data stored, the txt delimited file was imported to ArcPro GIS and a map with the basic infiltration rate was generated. The basic infiltration rates were then interpolated using ordinary kriging

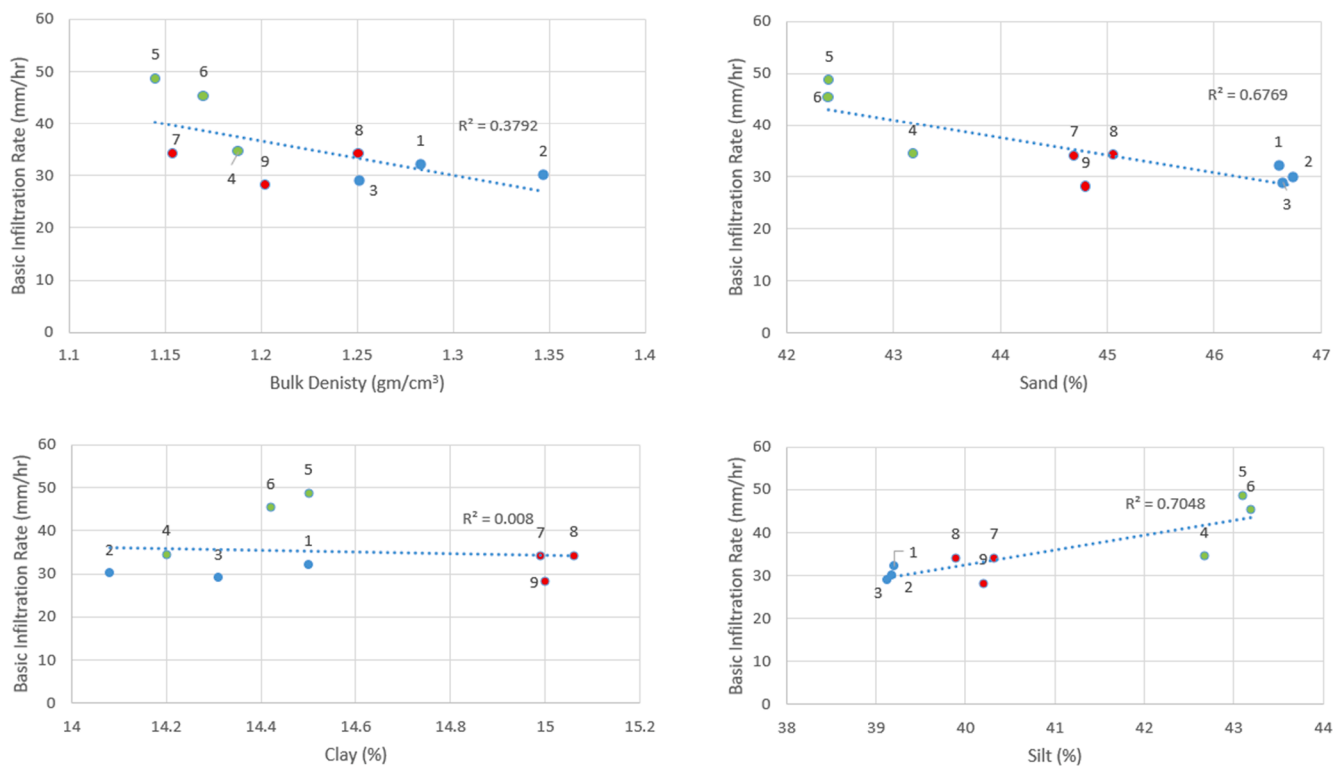


Fig. 12. The correlation between bulk density and texture with the measured basic infiltration rate in the head, middle and tail.

Table 2
The costs in dollars of the automated IoT-DRI.

Item	Unit	Quantity	Cost (\$)
(A) Automating system cost			
ESP32 (Wroom)	no	1	3
Real time clock module (DS3231)	no	1	1.5
SD Card module	no	1	0.5
SD card 32G	no	1	10
GPS module (GY-NEO6MV2)	no	1	5
Li-Ion batteries	no	5	15
Solar panel 12 V, 10A	no	1	20
MPPT solar charge controller	no	1	13
12 V DC $\frac{1}{2}$ " Solenoid valve	no	1	20
Miscellaneous (wires, battery case, holder, tape, hose ...etc.)			25
$\frac{1}{2}$ " Float valve	no	1	2
Total			115
(B) Other (same as traditional test)			
Commercial standard double ring infiltrometer	no	1	500
tank	no	1	70
Total	no	1	668

(Fig. 8). Ordinary Kriging is a spatial estimation method where the error variance is minimized. This error variance is called the kriging variance. It is based on the configuration of the data and on the variogram, hence is homoscedastic (Yamamoto, 2005). As Infiltration is highly impacted by spatial variability, interpolated maps cannot be used alone to determine infiltration in unmeasured points, and their dependability is case sensitive. However, in various case studies, irrigation systems design is being based on less measurement points, due to the infeasibility of proper infiltration mapping.

The points of entry were uploaded on ThingSpeak website in real time, to generate the infiltration curves of each point. The connection latency generates connection, a difference of 4–5 s between the data registration on the SD card and on the website. Fig. 9 shows the

infiltration curve of point no.1 as shown on the platform.

In order to validate the results generated by the prototype, the variation in water level with time was registered by using a stopwatch and a ruler, installed in the inner ring during the field operation of the prototype. Fig. 10 shows a comparison between the measured cumulative infiltration and the corresponding recorded data.

One of the main features resulted from automating DRI is the feasibility of investigating infiltration spatial variability. Although, the selected case study is relatively small (20×50 m), it showed significant variability in the middle of the field compared to the head and tail. The average basic infiltration of the head and tail were 30.44 and 32.19 mm/h with an StdDev = 1.27 and 2.8 respectively, on the other hand, the middle zone showed higher average basic infiltration rate of 42.87 mm/h and StdDev = 6.045 (Fig. 11). As mentioned before, basic infiltration rate is an essential feature in irrigation management especially in surface irrigation; such results spot the light on the spatial variability of soil infiltration regarding test sampling limitations even in small fields, thus magnifying the need of feasible automated infiltration measurement devices and higher resolution soil infiltration maps.

In an attempt to understand the weight of each feature on the basic infiltration rate under this case study, the correlation between the mapped soil features and the resulted basic infiltration rate was plotted. However, those results cannot be generalized due to the low number of tested points. In addition, out of the nine tested locations, two showed out of range results as compared to the rest. As shown in Fig. 12, sand and silt percentages showed the highest correlation to the spatial variability with $R^2 = 0.67$ and 0.7 respectively with almost no correlation with clay percentage, mainly due to the very low variation in clay percentage among the 9 samples (StdDev = 0.34). The same could be concluded for bulk density with a very low variation among the samples (StdDev = 0.063), however, bulk density reflected an expected trend, as in general higher bulk density means more compacted structure and lower infiltration rate.

The cost of the proposed prototype is relatively low as shown in table 2. The automation system components cost around 115\$ while the substantial cost is the one of the commercial standard DRI which was

relatively expensive > 500\$.

5. Conclusion

The advancement of cheap microcontrollers is revolutionizing IoT agricultural systems and creating low-cost innovative solutions for potential markets. This research work developed and field validated a falling head solar powered IoT-DRI, that proved its capability and reliability to measure, store and upload the infiltration rates in real time, and to turn off once the steady state is reached. The prototype is relatively cheap, the automation cost amounting to 115\$ (this cost does not include the ring itself nor the tank), easy to assemble, and the results could be accessed through ThingSpeak cloud service platform by any laptop or mobile device.

The automation rendered the multiple testing a feasible process, and the field measured infiltration data, collected in delimited Txt files, were imported to a Geographical mapping software to generate an interpolated map. The mapping results spot the potential error induced by the soil spatial variability. The middle of the field showed relatively higher variability compared to the head and tail, with a basic infiltration rate higher by 25%. Such results magnify the importance of considering an infiltration mapping/zoning approach for irrigation design and management. The proposed prototype will facilitate the investigation of the main drivers (soil properties) for such spatial variability in each case. In the discussed case study, sand and silt percentages showed the highest correlation with the basic infiltration rate $R^2 = 0.67$ and 0.7 respectively.

The potential applications of the device are not limited to agricultural applications, as DRI is widely used in various applications. The main challenge is related to the availability of reliable internet connection in the field, thus future enhancements of the device should include low-power wide-area network modulation techniques that do not depend on the internet availability.

Declaration of Competing Interest

The authors declare that they have no known competing financial interests or personal relationships that could have appeared to influence the work reported in this paper.

References

- Arriaga, F., Kornecki, T., Balkcom, K., Raper, R., 2010. A method for automating data collection from a double-ring infiltrometer under falling head conditions. *Soil Use Manag.* 26, 61–67.
- ASTM, 2018. ASTM D3385–18 Standard Test Method for Infiltration Rate of Soils in Field Using Double-Ring Infiltrometer. West Conshohocken, PA.
- Banerjee, S., Saini, A.K., Nigam, H., Vijay, V., 2020. IoT Instrumented Food and Grain Warehouse Traceability System for Farmers. In: 2020 International Conference on Artificial Intelligence and Signal Processing (AISP). IEEE, pp. 1–4.
- Bautista, E., Wallender, W., 1985. Spatial variability of infiltration in furrows. *Trans. ASAE* 28, 1846–1851.
- Brouwer, C., Prins, K., Kay, M., Heibloem, M., 1988. Irrigation water management: irrigation methods. *Train. Manual* 9.
- Constantz, J., Murphy, F., 1987. An automated technique for flow measurements from Mariotte reservoirs. *Soil Sci. Soc. Am. J.* 51 (1), 252–254.
- Dragonetti, G., Khadra, R., Daccache, A., Oubelkacem, A., Choukr-Allah, R., Lamaddalena, N., 2020. Development and application of a predictive model for treated wastewater irrigation management in a semiarid area. *Integr. Environ. Assess. Manage.* 16 (6), 910–919.
- Fatehnia, M., Paran, S., Kish, S., Tawfiq, K., 2016. Automating double ring infiltrometer with an Arduino microcontroller. *Geoderma* 262, 133–139.
- Gang, L., Xiangyun, W., 2008. Review on influential factors of soil infiltration characteristics. *Chin. Agric. Sci. Bull.* 7.
- García, L., Parra, L., Jimenez, J.M., Lloret, J., Lorenz, P., 2020. IoT-Based Smart Irrigation Systems: An Overview on the Recent Trends on Sensors and IoT Systems for Irrigation in Precision Agriculture. *Sensors* 20 (4), 1042. <https://doi.org/10.3390/s20041042>.
- Green, R.E., 1962. Infiltration of water into soils as influenced by antecedent moisture.
- Hino, M., Odaka, Y., Nadaoka, K., Sato, A., 1988. Effect of initial soil moisture content on the vertical infiltration process—A guide to the problem of runoff-ratio and loss. *J. Hydrol.* 102 (1–4), 267–284.
- Johnson, A.I., 1963. A field method for measurement of infiltration. US Government Printing Office.
- Lai, J., Ren, L.i., 2007. Assessing the size dependency of measured hydraulic conductivity using double-ring infiltrometers and numerical simulation. *Soil Sci. Soc. Am. J.* 71 (6), 1667–1675.
- Leonard, J., Andrieux, P., 1998. Infiltration characteristics of soils in Mediterranean vineyards in Southern France. *Catena* 32 (3–4), 209–223.
- Li, M., Liu, T., Duan, L., Luo, Y., Ma, L., Zhang, J., Zhou, Y., Chen, Z., 2019. The scale effect of double-ring infiltration and soil infiltration zoning in a semi-arid steppe. *Water* 11 (7), 1457. <https://doi.org/10.3390/w11071457>.
- Maheshwari, B.L., 1996. Development of an automated double-ring infiltrometer. *Soil Res.* 34 (5), 709. <https://doi.org/10.1071/SR9960709>.
- Mao, L., Bralts, V.F., Yinghua, P., Han, L., Tingwu, L., 2008. Methods for measuring soil infiltration: State of the art. *Int. J. Agric. Biol. Eng.* 1, 22–30.
- Milla, K., Kish, S., 2006. A low-cost microprocessor and infrared sensor system for automating water infiltration measurements. *Comput. Electron. Agric.* 53 (2), 122–129.
- Mohanraj, I., Ashokumar, K., Naren, J., 2016. Field monitoring and automation using IOT in agriculture domain. *Procedia Comput. Sci.* 93, 931–939.
- Pasha, S., 2016. ThingSpeak based sensing and monitoring system for IoT with Matlab Analysis. *Int. J. New Technol. Res.* 2.
- Prieksat, M.A., Ankeny, M.D., Kaspar, T.C., 1992. Design for an automated, self-regulating, single-ring infiltrometer. *Soil Sci. Soc. Am. J.* 56 (5), 1409–1411.
- Resch, C., Wahbi, A., 2016. Guidelines for Measuring Bulk Density of Soil.
- Reynolds, W., Elrick, D., Youngs, E., Amoozegar, A., Boolink, H., Bouma, J., 2002. 3.4 Saturated and field-saturated water flow parameters. *Meth. Soil Anal. Part 4*, 797–801.
- Sandoval, G.F.B., Galobardes, I., Teixeira, R.S., Toralles, B.M., 2017. Comparison between the falling head and the constant head permeability tests to assess the permeability coefficient of sustainable Pervious Concretes. *Case Stud. Constr. Mater.* 7, 317–328.
- Walker, W.R., Prestwich, C., Spofford, T., 2006. Development of the revised USDA-NRCS intake families for surface irrigation. *Agric. Water Manag.* 85 (1–2), 157–164.
- Yamamoto, J., 2005. Comparing ordinary kriging interpolation variance and indicator kriging conditional variance for assessing uncertainties at unsampled locations. In: Dessureault, Ganguli, Kecojevic, Dwyer, (Eds.), Application of computers and operations research in the mineral industry. Balkema.
- Youngs, E., 1987. Estimating hydraulic conductivity values from ring infiltrometer measurements. *J. Soil Sci.* 38, 623–632.
- Zhang, J., Lei, T., Yin, Z., Hu, Y., Yang, X., 2017. Effects of time step length and positioning location on ring-measured infiltration rate. *Catena* 157, 344–356.